Flexible Electronics

International Edition: DOI: 10.1002/anie.201501233
German Edition: DOI: 10.1002/ange.201501233

# Transparent Electrodes Printed with Nanocrystal Inks for Flexible Smart Devices

*Jizhong Song and Haibo Zeng**

light-emitting diodes · nanocrystal inks · nanotechnology · thin films · transparent electrodes

*Transparent electrodes (TEs) are crucial in a wide range of modern electronic and optoelectronic devices. However, traditional TEs cannot meet the requirements of smart devices under development in unique fields, such as electronic skins, wearable electronics, robotic skins, flexible and stretchable displays, and solar cells. Emerging TEs printed with nanocrystal (NC) inks are inexpensive and compatible with solution processes, and have huge potential in flexible, stretchable, and wearable devices. Every development in ink-based electrodes makes them more competitive for practical applications in various smart devices. Herein, we provide an overview of emergent ink-based electrodes, such as transparent conducting oxides, metal nanowires, graphene, and carbon nanotubes, and their application in solution-based flexible and stretchable devices.*

## 1. Introduction

Currently, the commercially used transparent electrodes (TEs) in classical optoelectronic devices, such as light-emitting diodes (LEDs), solar cells (SCs), and photodetectors (PDs), are made of indium tin oxide (ITO), which is usually deposited by vacuum sputtering. There are serious problems associated with the use of such electrodes in terms of sustainable development for both technical and economic reasons.[1] First, indium is a rare metal. It is becoming more and more expensive owing to its ever-increasing consumption and predictions that indium resources will be exhausted within ten years. Therefore, the search for cheaper and more abundant substitutes is imperative.[2] Second, the vacuum-sputtering technique, which is conducted in a vacuum at high operating temperatures, usually wastes more than half of the ITO source (more than 70% of the ITO ejected from a target is deposited on the walls of the sputtering chamber), and is thus not compatible with the current demand for low-cost optoelectronic devices.[3] Furthermore, the emergence of smart optoelectronics, such as flexible, stretchable, and wearable devices are receiving more and more attention, and such devices require new TEs.[4] ITO is not ideal for these highly flexible electronics owing to its brittleness. Cracks generated as a result of mechanical bending or stretching seriously deteriorate the electrical properties of the film. TEs based on nanocrystal (NC) inks can be processed by low-cost printing techniques, which are compatible with the flexible and stretchable substrates[5] and can also reduce the consumption of the raw materials. Therefore, films assembled from NC inks have received increasing attention as next-generation TEs for optoelectronic devices.

NC inks are typically nanomaterials that are dispersed in various solvents and can be assembled into films through solution processes. The expanding range of NC inks includes transparent conducting oxides (TCOs), metal-nanowire (NW) networks, graphene, and carbon nanotubes (CNTs; Figure 1a). The motivation for developing these NC inks includes several aspects. First, the assembly of NC films deposited by solution-based processes can effectively lower the cost of thin-film electronics by reducing raw-material consumption. Second, TEs based on NC inks can be assembled through facile printing techniques, such as ink-jet printing and roll-to-roll production, as well as solution processes, including spin-coating, spraying, and metering-rod techniques (Figure 1b). The use of these printing technologies during the fabrication of optoelectronics has raised interest in both academic and industrial communities. Printing technologies are promising for the low-cost and high-

[*] J. Z. Song, Prof. H. B. Zeng
State Key Laboratory of Mechanics and Control of Mechanical Structures, College of Materials Science and Technology, Nanjing University of Aeronautics and Astronautics
Nanjing 210016 (China)
J. Z. Song, Prof. H. B. Zeng
Institute of Optoelectronics and Nanomaterials, Herbert Gleiter Institute of Nanoscience, School of Materials Science and Engineering, Nanjing University of Science and Technology
Nanjing 210094 (China)
E-mail: zeng.haibo@njust.edu.cn

throughput manufacture of solution-based, light-weight electronic devices, such as flexible displays, lighting, PDs, and SCs. For some new flexible and stretchable technologies, TEs based on NC inks offer compelling capabilities. For example, flexible optoelectronics, such as flexible displays and flexible SCs, ideally require the large-area manufacture of devices based on patterned films that can be controllably processed by ink-jet printing and roll-to-roll production. The low-cost manufacturing of NC-ink-based TEs on soft substrates is also beneficial for the creation of smart electronics, such as stretchable displays and wearable electronics that are foldable, rollable, environmentally benign, and recyclable. Examples of some highly anticipated smart optoelectronic devices are shown in Figure 1 c. TEs based on NC inks have fueled the development of a wide range of potential smart applications, such as low-cost solution-processed optoelectronics, flexible and stretchable displays, wearable electronics, and electronic skins. Thus, a new era in integrated smart technologies founded on NC-ink-based TEs is emerging.

Rapidly growing markets for flexible TEs, a far-reaching technology used in a myriad of common applications, include touch screens, flexible displays, printable electronics, solid-state lighting (especially organic LEDs (OLEDs)), and photovoltaics for renewable-energy applications.[6] Herein, we review the progress, prospects, and contemporary challenges associated with NC-ink-based flexible and stretchable TEs.

## 2. Transparent Electrodes Printed with Nanocrystal Inks

Owing to the small size of NCs, the assembled films can provide a highly conducting path with a high light transmittance. The NC materials can be solubilized in various solvents by fairly straightforward and inexpensive techniques and then serve as inks. NC inks can be cast into films by solution processes that do not require high temperatures, a high vacuum, or expensive processes and that avoid low-throughput production during the fabrication of TEs. These methods are compatible with the existing roll-to-roll coating equipment and infrastructure used in the ink and paint coating industries. The combination of inexpensive starting materials, high-volume and inexpensive printing techniques, superior mechanical flexibility, and potential applications in unique optoelectronic devices spurs continued research into these NC inks in both industry and academia.

Several emerging nanoscale materials show great promise as TEs. These materials include nanoscale forms of TCO NCs, metal NWs, CNTs, and graphene. The utility of these materials as TEs stems largely from their intrinsically high conductivity, which enables the assembled optically transparent films to have appropriate conductivity. The typically high aspect ratio and the unique shape of NCs yield films with adequately low resistance and superior mechanical flexibility. These properties in combination with the low-cost materials and film-processing techniques make emerging NC inks very attractive for use as TEs in smart optoelectronic devices.

### 2.1. Metal-Oxide Nanocrystal Inks

TCOs are a group of well-known wide-band-gap metal-oxide materials that are both optically transparent and electrically conductive for use as TEs in various optoelectronic devices. Typical examples include ITO, fluorine-doped tin oxide (FTO), and aluminum-doped zinc oxide (AZO). Mainstream scientific studies and current industrial technologies mainly rely on vacuum-sputtering processes, which cannot be readily used to control the patterns of ITO films on flexible substrates and have a production yield generally lower than 30%. Thus, there has been increasing interest in and an urgent need for alternative deposition processes and TE materials to replace conventional ITO electrodes. The requirements for next-generation TEs are mainly that they should be cheap, flexible, and compatible with large-scale manufacturing methods for optoelectronic devices.

The deposition of TCO NCs from the solution phase is a promising alternative to sputtering for the fabrication and patterning of TEs.[7] Kim and co-workers demonstrated the deposition of various doped oxides, including zinc- and tin-codoped $In_2O_3$ (IZTO),[8] ITO,[9] and titanium-doped $In_2O_3$ (TIO),[10] through the dispersion of nanoparticle powders. The printed films have broad application as TEs in liquid-crystal devices (LCDs) and organic solar cells (OSCs) without the use of any conventional photolithography processes, thus indicating that the printing of patterned TEs is a viable alternative to the sputtering of ITO TEs for various solution-based optoelectronic applications. These TEs are a promising cost-effective alternative owing to the absence of photo-

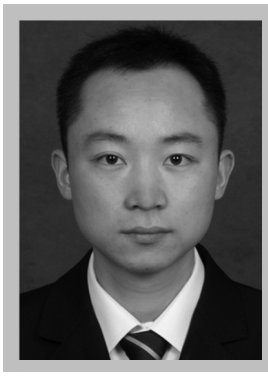

*Jizhong Song received his Bachelor's degree from the School of Materials Science and Engineering at Shanghai University in 2011. He is currently pursuing his PhD under the supervision of Professor Haibo Zeng at Nanjing University of Aeronautics and Astronautics. His current research focuses on doped colloidal nanocrystal inks and their applications in solution-based flexible and stretchable organic/inorganic hybrid photodetectors and light-emitting diodes.*

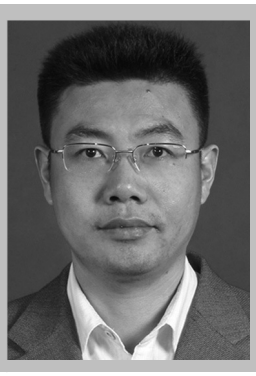

*Haibo Zeng is director of the Institute of Optoelectronics and Nanomaterials at Nanjing University of Science and Technology (NUST). He received his PhD degree from the Chinese Academy of Sciences (CAS) in 2006 then worked at CAS, the University of Karlsruhe (Germany), and the National Institute for Materials Science (Japan). In 2013, he moved to NUST and established a Nano-optoelectronics group. His research focuses on optoelectronics based on nanocrystals and two-dimensional semiconductors.*

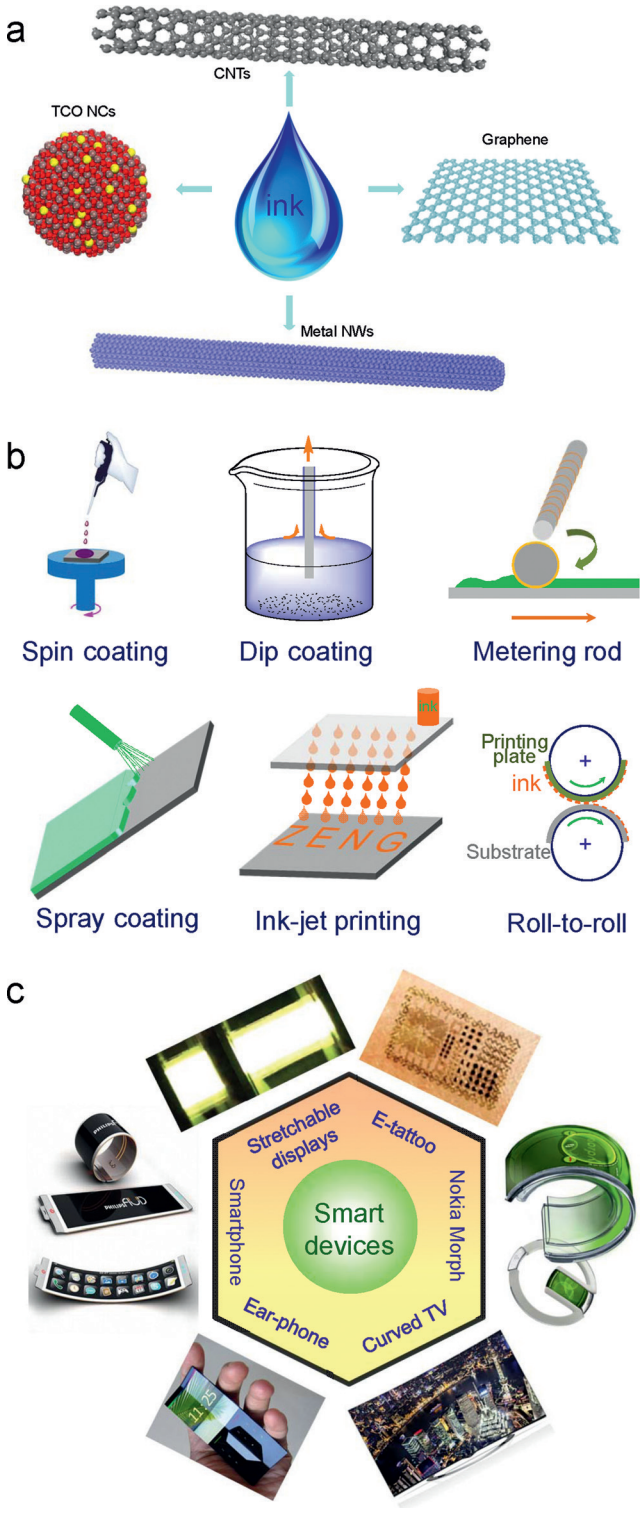


***Figure 1.*** Classes of NC inks, solution-processing techniques, and examples of smart optoelectronics. a) Three-dimensional illustrations of various NC materials that can serve as inks. b) Depiction of various solution deposition methods. c) Nanocrystal-ink-based TEs used in modern smart systems. Images of an e-tattoo (courtesy of N. Lu, University of Texas at Austin), the Morph of Nokia, a curved LED television screen of the company LG, a Philips earphone and smartphone, and a stretchable display (courtesy of Q. B. Pei, University of California).

lithography processes for patterning and efficient raw-material usage.

However, ultrasonic dispersion of the oxide powder is not an optimal method for the use of solution-processed inks. The synthesis of TCO NCs from the solution phase is a promising method for the fabrication and patterning of TCO films. The synthesis from solution leads to the formation of well-dispersed TCO NCs with controlled size, morphology, and composition. The resulting high-performance TCO NC inks are compatible with flexible and stretchable substrates and can be used to deposit a film in a straightforward way by solution-based techniques and to directly pattern TE layers. Therefore, printed TEs can be of great value for application in various smart devices, such as OSCs, LCDs, OLEDs, and touch screens.[11]

An effective method for the fabrication of high-quality TCO NC inks with high solution stability and dispersibility is highly desirable, as is a well-crystallized structure. Bühler et al. reported a liquid-based synthesis of ITO NCs with good electrical properties; however, these NCs were difficult to deposit as a thin film.[12] AZO[13] and ITO[14] NCs were synthesized with simultaneous control of their size and doping level by the hot-injection method. These NCs were used to assemble uniform NC films by spin casting on centimeter-wide glass substrates. The ITO NC film with a thickness of 146 nm became conductive and transparent with a sheet resistivity of 356 $\Omega\,sq^{-1}$ and a transparency of 93% in the visible spectral range upon thermal annealing at 300 °C for 6 h under an atmosphere of Ar and 5% $H_2$. The reported synthetic and assembly processes provide a promising approach to the preparation of solution-based NC films on flexible substrates.

Various synthetic methods have been developed for the straightforward preparation of commercial NCs by controlling the reaction temperature and precursor. Murray and co-workers reported a general synthesis of a family of n-type TCO NCs through doping with aliovalent cations.[15] The NCs were synthesized by a rapid nucleation process at a high temperature (> 300 °C) through the decomposition of metal-carboxylate precursors. These reactions bear some challenges for producing NCs with specific structures and compositions. They are sensitive to variations in temperature and reagent mixing, thus making it difficult to control the reaction conditions and reproduce the syntheses.

Ito et al.[16] developed a high-yielding synthetic method at lower temperature that produced crystalline, monodisperse NCs below the thermal-decomposition temperature of the precursors. Slow injection of the metal oleate complex into the solvent oleyl alcohol at 230 °C triggered a rapid esterification reaction. The method can be applied to a wide range of NCs, including ITO, iron oxide ($\gamma$-$Fe_2O_3$), and ZnO.

NCs can also be synthesized by hot injection, which has been very popular in recent years for the synthesis of colloidal NCs. The fabrication process, which involves a chemical reaction between the injected source and the mother solution in a very localized environment, has two disadvantages.[17] First, as a small injection dose is usually adopted to promote high-quality doping, the ability to scale up the process is limited. Second, the doping quality is very sensitive to the

injection parameters and dopant. Therefore, all parameters need to be explored and changed again for the preparation of other NCs. The poor applicability of the approach has greatly hindered the production of various NC inks in high yield for industrial applications.

Recently, Song et al.[18] reported a facile and universal one-pot method for the synthesis of a wide range of TCO NCs and the corresponding NC electrodes, which showed high performance in solution-based devices (Figure 2a–d). The proposed approach is general for various TCOs, as well as other oxide (e.g. CoO, MnO, $Fe_3O_4$, CdO) NCs. As it is a one-pot method, it can be readily scaled up to a 10 g synthesis. The TCO NCs (Figure 3) are characterized by high crystallinity, uniform morphology, monodisperse size, effective doping, and colloidal stability over 1 year and hence can be used as inks to print smooth, crack-free, highly transparent, and conductive films. The formed NC electrodes had a surface roughness as low as 1.6 nm. Typically, a 300 nm thick NC film had a resistivity of just 112 $\Omega\,sq^{-1}$ and a transparency as high as 87% and thus exhibited better performance than other reported films. The NC TEs can drive solution-based PLEDs with luminance as high as 2200 $cd\,m^{-2}$ at a current density of 100 $mA\,cm^{-2}$.

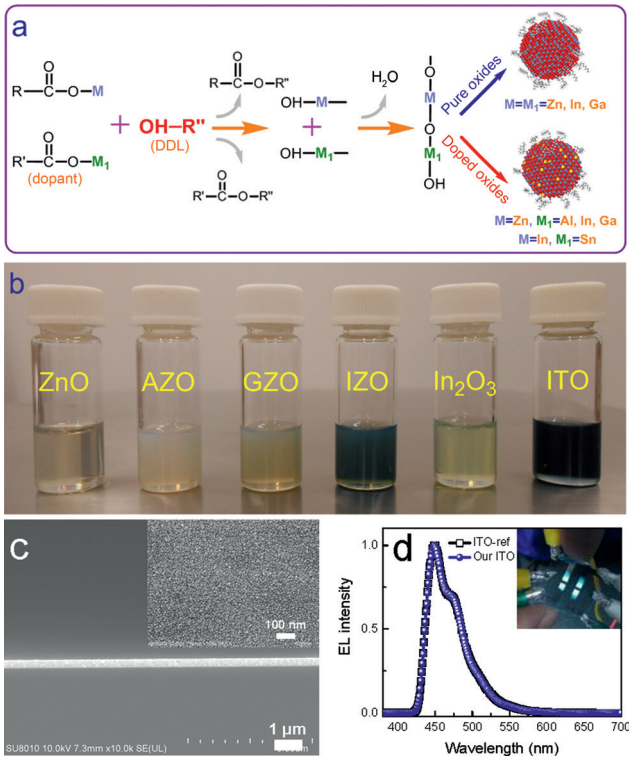


***Figure 2.*** TCO-based NC inks for TEs in LEDs. a) Synthesis of pure and doped NCs. b) Photograph of a series of NC inks with a stability of more than a year. c) Cross-sectional and top-surface SEM images of a three-layered NC electrode. d) EL spectra of PLEDs with assembled ITO NC TEs and commercial ITO. Inset: photograph of the device emitting blue light.

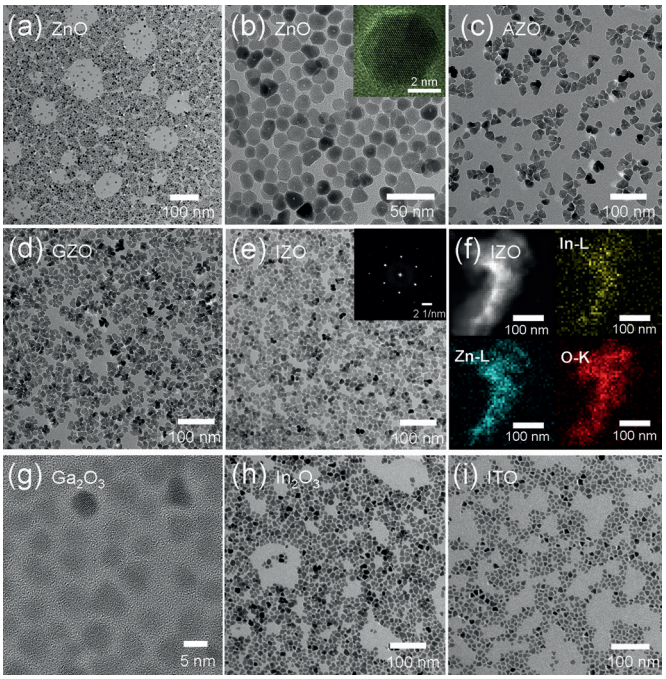


***Figure 3.*** SEM images of various TCO NCs synthesized by a one-pot method.

Della Gaspera et al. studied the non-injection synthesis of ZnO-based NCs. The simple synthetic method is reproducible for the creation of nearly monodisperse colloids and can be performed at high concentrations with near-unity reaction yields. High doping levels of over 15% are possible. These advances represent a step forward towards harnessing the potential of solution processes for the development of next-generation TEs.[19] Niederberger and co-workers explored the wet-chemical deposition of ATO NCs into films.[20] They demonstrated that these films have the required high quality for use as TEs in optoelectronic devices. To demonstrate that these films are indeed viable as TEs, they showed that an OLED fabricated on an ATO-NC-based TE exhibited an electrical and optical performance comparable to that of commercially available ITO.

Generally speaking, the electrical properties of TEs based on TCO NC inks are not optimal for various optoelectronic devices. At present, two strategies have been proposed to enhance their electrical performance. Martucci and co-workers proved that UV treatment could remove organic compounds and reduce interparticle resistance to increase the free-carrier concentration and enhance electrical conductivity.[21] The electrical resistance of the NC assemblies is about 30 $k\Omega\,sq^{-1}$ for the as-deposited films. It drops down to 300 $\Omega\,sq^{-1}$ after UV treatment. Short-ligand exchange is also an effective approach to improve the electrical properties of the assemblies. Sun and co-workers reported that ITO NCs were synthesized and stabilized with organic ligands.[22] These long-chain surfactants were readily replaced with tetrabutylammonium hydroxide (TBAOH) to form a stable methanol dispersion. The original ITO NC assemblies showed high transparency (>88%) and low resistivity ($2.6\times10^{-3}\,\Omega\,cm$).

The conductivity of the NC films was doubled by short-ligand exchange. The surface modification of TCO NCs with a volatile surfactant, followed by film deposition, is an effective strategy for fabricating films in a solution process with the desired transparency and conductivity for TE applications.

### 2.2. Metal-Nanowire Inks and Assembled TEs

Recently, considerable attention has been paid to potential applications of TEs derived from metal-nanowire inks, such as wearable electronics, robotic skins, implantable medical devices, flexible and stretchable displays, OLEDs, and OSCs.[23] Random NW networks with high transparency and electrical conductivity can be used as flexible and stretchable electrodes in these innovative devices.[24] In particular, metal-nanowire inks exhibit huge potential owing to their straightforward preparation by solution-processing techniques, such as spray coating,[25] drop casting,[26] spin coating,[27] vacuum filtration,[28] and rod coating.[29] All these techniques are compatible with low-temperature deposition processes without the need for any vacuum equipment.

#### 2.2.1. Silver-Nanowire Inks

At present, their superior conductivity and intrinsic flexibility make Ag NWs especially promising for integration with elastomers. Impressive progress has been made with the corresponding flexible and stretchable electrodes. A typical method for the synthesis of Ag NWs is the reduction of silver nitrate in the presence of poly(vinylpyrrolidone) (PVP) in ethylene glycol as the reaction medium and reductant.[30] The as-obtained NWs can be dispersed in various solvents, such as water, ethanol, and isopropyl alcohol, to form an ink for the assembly of TEs through facile solution-based processes. Xu and Zhu reported a highly conductive and stretchable Ag NW/poly(dimethylsiloxane) (PDMS) conductor prepared by the infiltration of the PDMS prepolymer into a thick layer of Ag NWs and thermal curing. The conductor exhibited high stretchability and a conductivity of 8130 $S\,cm^{-1}$ (0.24 $\Omega\,sq^{-1}$) at $\varepsilon = 0\,\%$ and 5285 $S\,cm^{-1}$ at 50 % strain.[4a] Akter and Kim reported the creation of highly adhesive transparent and stretchable coatings by the spray deposition of Ag NWs on a polydopamine-modified stretchable elastomeric substrate.[31] Similarly, Lee et al. illustrated a novel concept to enhance the permanent and close attachment of Ag NWs to a PDMS substrate by silane modification.[32] The Ag NW elastomers maintained high transparency (87 %) and a high conductivity (27 $\Omega\,sq^{-1}$) and showed excellent mechanical durability, flexibility, and stretchability.

Owing to their low sheet resistance and high transparency, electrodes based on Ag NWs are good candidates for device integration in existing applications. Their mechanical properties also provide opportunities for integration in emerging flexible and stretchable devices, such as SCs,[25b,33] LEDs,[34] and PDs.[35]

Kim and co-workers reported the cost-efficient brush painting of all-solution flexible OSCs (Figure 4).[36] Kang and co-workers fabricated highly efficient and bendable OSCs with Ag NWs as TEs by spin coating.[37] The Ag NW networks fabricated by the solution process were highly transparent (95 % transmittance at 550 nm), highly conductive (10 $\Omega\,sq^{-1}$), and highly flexible, thus proving that the solution technique is a promising low-cost and fast process for the fabrication of OSCs. Brabec and co-workers explored the all-solution fabrication of parallel tandem SCs by using Ag NWs as an intermediate charge-collecting electrode.[38] The resulting cells have a high fill factor of approximately 60 % with enhanced current densities, which are identical to the sum of the current densities of the subcells. These results suggest that solution-processed Ag NWs have huge application potential in SCs.

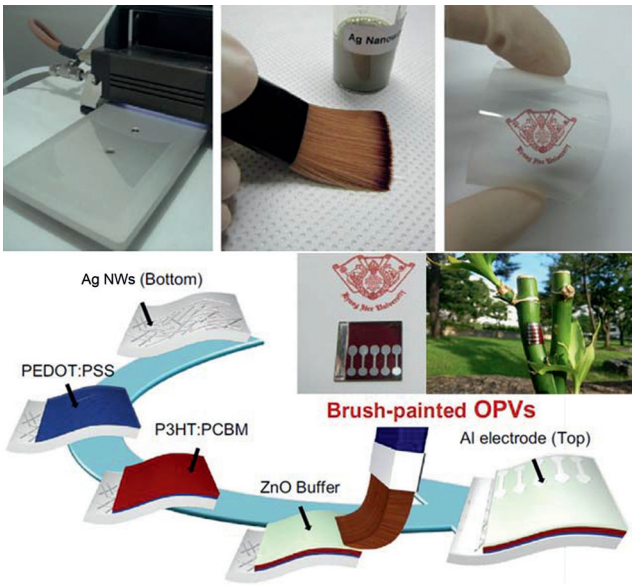


***Figure 4.*** Photographs and schematic illustration of the brush painting of an Ag NW ink on a PET substrate for OSCs.

Flexible and stretchable displays and solid-state lighting systems would enable the development of expandable and foldable screens for smartphones, electronic clothing, and rollable or collapsible wallpaper-like lamps.[39] Yu et al. first demonstrated that a composite electrode in which the Ag NWs were embedded in a cross-linkable polyacrylate substrate could successfully replace the traditional ITO glass substrate (Figure 5 a).[40] This result opened up the possibility of producing high-flexibility and high-performance devices. Gaynor et al. demonstrated that solution-processed Ag NW/PMMA composite electrodes were suitable for large-area OLEDs.[41] The efficiency and color stability of white-light LEDs fabricated on these electrodes are similar to those of devices based on commercially used ITO (Figure 5 b). Liang et al. reported an elastomeric polymer-based Ag NW substrate with yellow-light LEDs consisting of ethoxylated trimethylolpropane triacrylate, poly(ethylene oxide), and lithium trifluoromethanesulfonate. The efficiency was kept at 2.5 $cd\,A^{-1}$ under 120 % strain (Figure 5 c,d).[42] The fabrication process is quite facile and scalable and could therefore be readily adapted to the demonstration of a simple passive-matrix display. The display retained the rubbery elasticity of

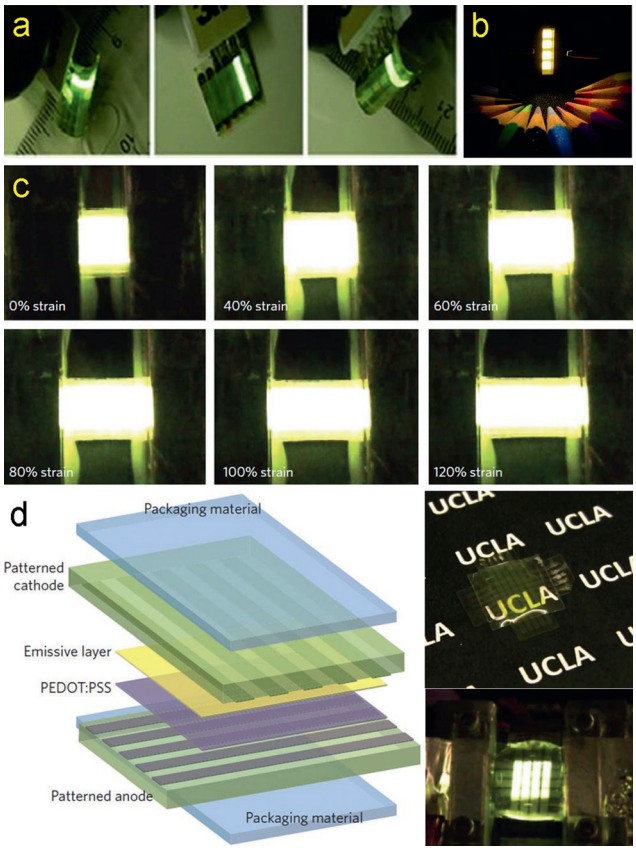


***Figure 5.*** a) Photographs of shape-memory PLEDs emitting with 300 cd m$^{-2}$ efficiency. b) Photographic image of four operating Ag NW OLEDs. c) Photographs of a PLED (original emission area, 5.0×4.5 mm$^2$) biased at 14 V at specified strains. d) Schematic illustration and photograph of an encapsulated fully stretchable PLED display comprising 5×5 pixels.

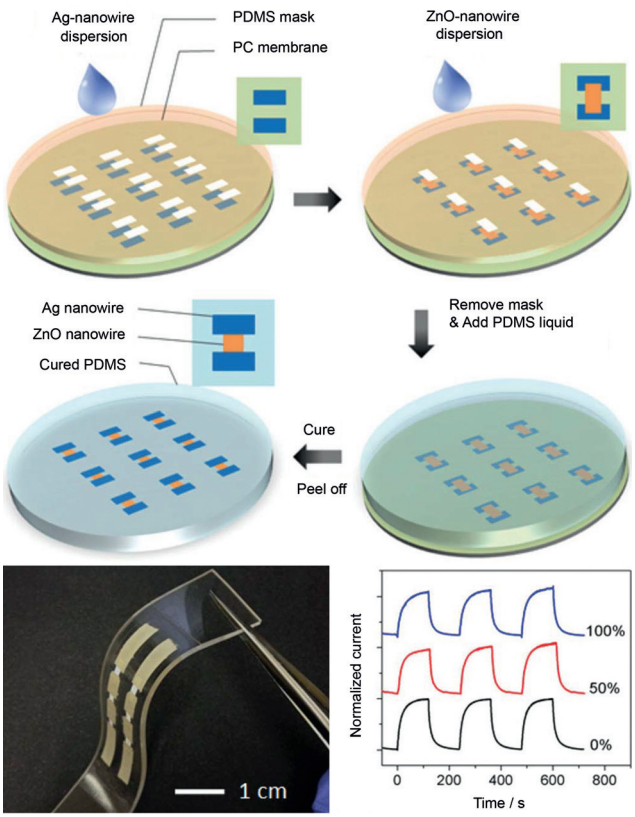


***Figure 6.*** Lithographic filtration method for the fabrication of stretchable all-nanowire PD arrays, photograph of such a PD array, and switching behavior of a stretchable device with three PDs connected in series.

the individual PLED pixels. This advance is an important step towards fully stretchable electronics. Along with the future development of elastomeric thin-film transistors, rubbery sealing materials, and stretchable light-emitting polymers, fully stretchable active-matrix OLEDs for the high-resolution display of information are anticipated in the near future.

PDs are a type of electronic device for sensing light. They have found broad application in consumer electronic devices, such as digital cameras. Flexible and stretchable PDs could even be implanted in human eyes. One could then take digital images by simply blinking. Such implantable PDs could also help blind people to regain their visual senses.[43] Lee and co-workers reported all-solution-processed, stretchable NW PDs prepared by a spray-coating[44] or filtration method.[43] The stretchable Ag/ZnO/Ag NW PDs showed excellent cycling and mechanical stability (Figure 6) with no obvious performance degradation after 50 repeated stretching cycles and scotch-tape tests. The fabrication method can be readily extended to a wide range of NW PDs, which may find application in future stretchable, wearable, and implantable electronics.

### 2.2.2. Copper-Nanowire Inks

Cu NWs are a less expensive alternative to Ag NWs, because Cu is at 100 times cheaper and 1000 times more abundant than Ag. Furthermore, Cu NWs have nearly the same conductivity as Ag NWs with a sheet resistance below 100 Ω sq$^{-1}$. Therefore, the use of Cu NW ink has become popular in recent years in studies towards the development of flexible and stretchable TEs.[45] Cu NW inks have been synthesized by two general approaches: ethylenediamine (EDA)-mediated and alkylamine-mediated synthesis. The EDA-mediated synthesis of Cu NWs was reported for the first time by Zeng and co-workers[46] and modified by Rathmell et al., who scaled up the reaction by a factor of 100.[47] The Cu NWs were (90 ± 10) nm in diameter and (10 ± 3) μm in length with spherical particles attached to one end (Figure 7a). The diameter and the growths on one end are not favorable for the photoelectric properties of the NWs. High-quality Cu NWs cannot be obtained easily by the EDA-mediated method.

The alkylamine-mediated method can be used to synthesize high-quality and uniform Cu NWs.[48] The as-obtained Cu NWs with a high aspect ratio (diameters of about 18 nm and lengths up to 40 μm) provide a long pathway for electron transport and a large space for light transmission (Figure 7b). TEs fabricated with the Cu NW ink had a low sheet resistance

  

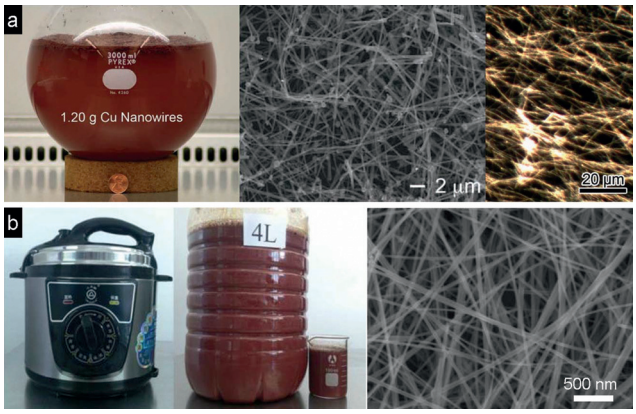


***Figure 7.*** Cu NW inks for TEs. a) Photograph of the reaction flask after the growth of Cu NWs (1.20 g), and SEM and optical images of the Cu NW product. b) Commercial electric pressure cooker used for the synthesis of Cu NWs, and SEM image of as-prepared Cu NWs.

of 51 $\Omega\,sq^{-1}$ at 93% transmittance.[48a] An elastomeric composite TE comprised of a percolation network of Cu NWs embedded in the surface layer of an elastomeric polyurethane matrix has been fabricated. The composite electrodes exhibited a low sheet resistance of less than $10^2\ \Omega\,sq^{-1}$ at tensile strains up to 60%. High stretchability was observed in a wide range of strain rates over 200 cycles of stretching.[49]

However, Cu NW conductive films have a serious shortcoming for future practical use in flexible and stretchable optoelectronics. The main obstacle is the lack of stable conductivity, because copper is more sensitive to oxygen and moisture than other noble metals. Many researchers have developed strategies to enhance the stability of NW films.[50] Wiley and co-workers proposed nickel shell-coating as an effective way to improve the oxidation resistance of Cu NWs.[50a] They added the synthesized Cu NWs to an aqueous solution of $Ni(NO_3)_2$ to enable the growth of Ni shells. Won et al. reported oxidation-resistant copper-nanowire-based composite electrodes that are highly transparent, conductive, and flexible.[50c] First, treatment with lactic acid effectively removed both the organic capping molecule and the surface oxide/hydroxide from the Cu NWs, thus allowing direct contact between the NWs. The subsequent embedding of the Cu NWs in AZO dramatically improved their thermal stability and oxidation resistance (Figure 8). These Cu-NW@AZO composite electrodes exhibited high transparency (83.9% at 550 nm) and a low sheet resistance (35.9 $\Omega\,sq^{-1}$). Their performance was maintained even after bending 1280 times with a bending radius of 2.5 mm. The CuNW@AZO electrodes showed a power conversion efficiency (PCE) of 7.1%, which is comparable to that of conventional ITO TEs.

These two-step methods are difficult to scale up for industrial production. More seriously, the completely heterogeneous protection induced ambiguous interfaces, thus limiting the improvement of stability and conductivity. In contrast to the previously suggested two-step method, a one-pot method was developed to synthesize Cu NWs with $Cu_4Ni$ alloying shells.[51] Such consecutive growth and in situ surface alloying enabled the preparation of Cu NWs that were more than 50 μm long with smooth surfaces and highly crystalline

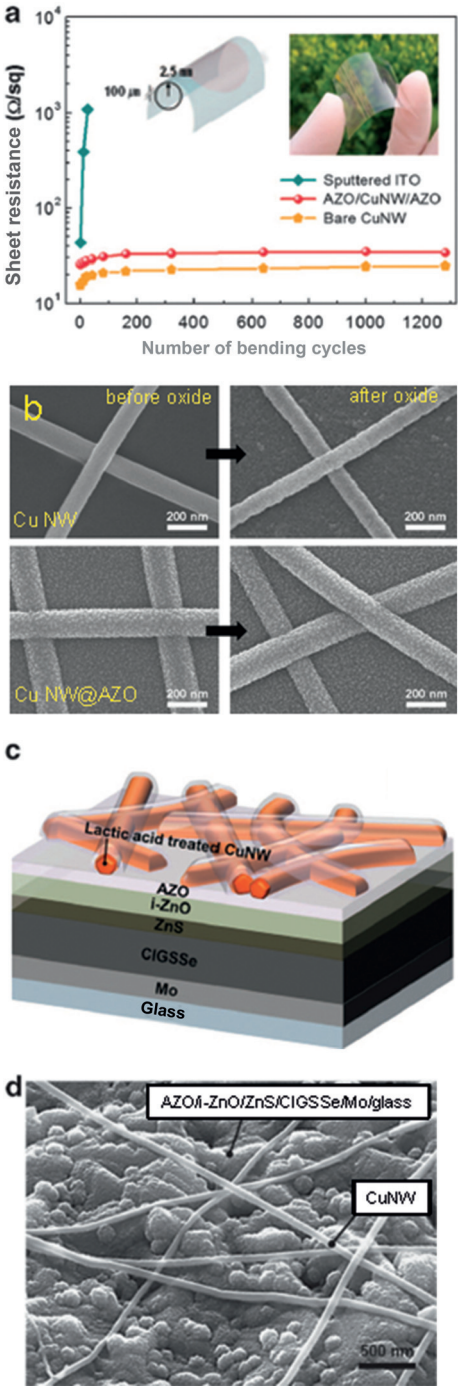


***Figure 8.*** a) Changes in the sheet resistance during bending tests of NW electrodes. b) SEM images showing the morphological change in the NWs upon thermal oxidation. c) Structure and d) surface SEM image of a solar cell with a Cu NW@AZO composite TE.

alloying shells with clear and abrupt interfaces (Figure 9). By embedding Cu@Cu–Ni NWs into PDMS, new elastomers were formed that exhibited high performance with a transparency of 80% and a resistance of 62.4 $\Omega\,sq^{-1}$: properties that are superior to those of typical ITO/PET.

Significantly, the stable lifetime of these elastomers is estimated to exceed 1200 days in the natural environment. In

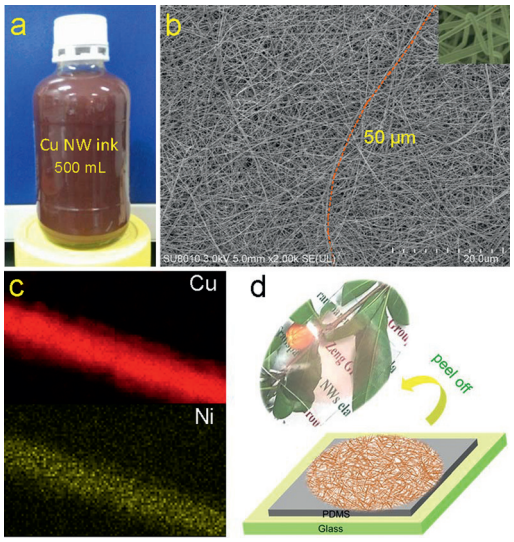


***Figure 9.*** a) Photograph of a high-quality Cu@Cu–Ni NW ink redispersed in hexane. b) SEM image of as-obtained NWs with lengths of more than 50 μm. c) Elemental mapping of a single alloy NW. d) Schematic illustration (gray layer: PDMS; green layer: glass) and photograph of a nanowire–elastomer composite.

addition to an outstanding ability to resist oxidation, these elastomers exhibit highly stable conductivity under extreme bending and stretching conditions. Thus, OLEDs with Cu@Cu–Ni NWs as conductors were stable for 600 cycles (Figure 10a).[51] Won et al. described the fabrication without annealing of stretchable TEs based on Cu NWs through a simple and scalable process at a low temperature without a vacuum. The reversible and extremely stretchable (up to 700% strain) helical NWs have potential for application as stretchable TEs (Figure 10b).[52] Flexible and stretchable TEs based on a copper-nanowire percolation network could be used in various smart devices.[53]

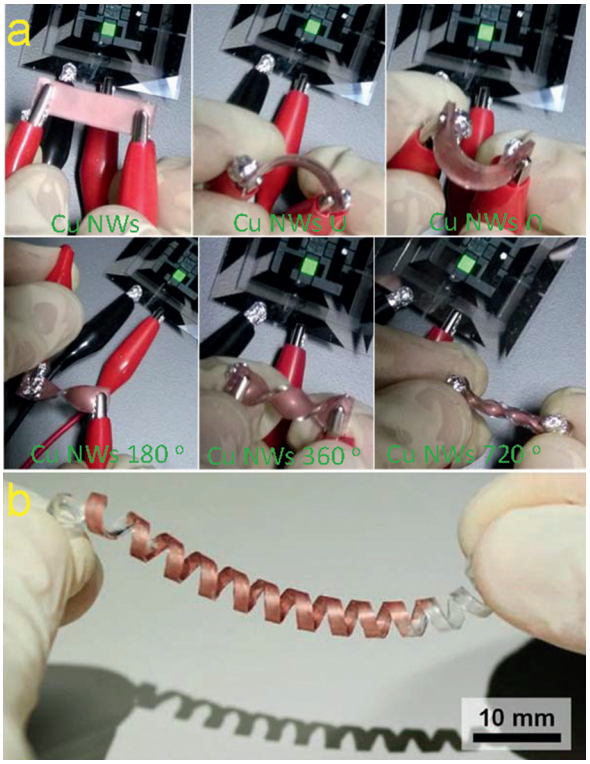


***Figure 10.*** Cu NW stretchable TEs. a) Photographic images of working OLEDs with Cu@Cu–Ni NW conductors under various strains. b) Photograph of the helical Cu NW electrodes.

The reports on Cu NW inks as TEs for optoelectronics are few as compared to those on Ag NWs. Im et al. reported the first high-performance TE with embedded Cu NWs for typical flexible OLEDs. The as-obtained NW TEs showed outstanding oxidation stability, an exceptionally smooth surface topography, and excellent optoelectrical performance (Figure 11).[54]

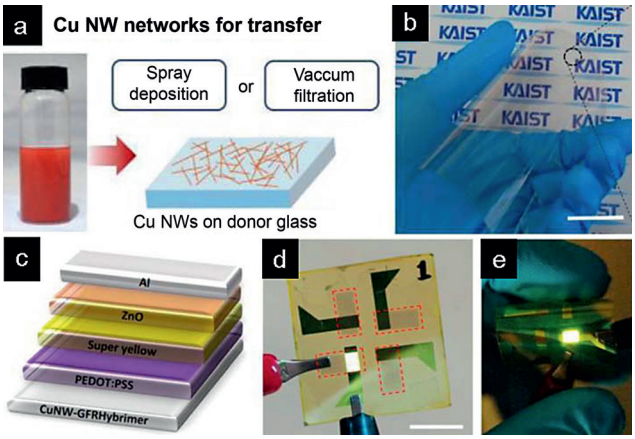


***Figure 11.*** a) Fabrication of a Cu NW film. b) Photograph of the Cu NW film. c) Demonstration of the flexible OLED device structure (layers from the top: Al, ZnO, Super Yellow, PEDOT:PSS, Cu NW–GFRHybrimer). d,e) Photographs of the device operating in the flat state (d) and the flexed state (e).

### *2.3. Graphene Inks*

Graphene, an atomically thin, planar membrane of carbon, is a zero-bandgap semiconductor possessing room-temperature mobility on the order of $10^4\,cm^2\,V^{-1}\,s^{-1}$ with a carrier concentration of up to $10^{13}\,cm^{-3}$. These electronic properties endow it with exceptional in-plane conductivity, so that graphene has a rather low sheet resistance even though it has a thickness of only a single atomic layer (0.34 nm). Light transmission through a thin graphene stack can be estimated to be $(100-2.3\,N)\%$ and the sheet resistance of a doped layer of graphene scales as $62.4\,\Omega\,N^{-1}$, in which $N$ is the number of graphene layers[1b].

The two-dimensional sheets of $sp^2$-hybridized carbon atoms have very high conductivity and are nearly transparent. Recent advances in the synthesis and characterization of graphene indicate that it may be the most promising material for the fabrication of TEs by solution processes.[55] Liquid-based suspensions of graphene could be ideal for coatings because low-cost methods, including spin coating, roll-to-roll processing, and printing, could be used. Recent reports

suggest that the solution processing of graphene films has great potential for transparent conducting technologies.

Bulk graphite can be separated into single atomic planes by a known exfoliation process. The chemical exfoliation of graphite in solution[56] is one potential approach to the large-scale production of graphene and has the advantage from a manufacturing standpoint that it leads to the solution-phase processing of a graphene "ink". This method enables the fabrication of TE films by high-speed printing. Dai and co-workers first produced high-quality, single-layer graphene sheets stably suspended in organic solvents by chemical exfoliation.[57]

Blake et al. demonstrated that large-scale TEs can be obtained by spray coating the suspended graphite fabricated by sonicating bulk graphite in *N*,*N*-dimethylformamide (DMF).[58] This method yields a suspension of thin graphitic platelets with a large proportion of monolayer graphene flakes. However, these 90% transparent films have a resistivity of up to 5 $k\Omega\,sq^{-1}$, which makes the method unrealistic for the commercial fabrication of TEs. Dai and co-workers obtained graphene suspended in DMF by using the surfactant DSPE–mPEG. They demonstrated successful film growth through Langmuir–Blodgett (LB) assembly.[57a] The film had a resistance of approximately 8 $k\Omega\,sq^{-1}$ with a corresponding transparency of approximately 83%. Similarly, De et al. demonstrated a simple approach of sonicating graphite powder in a solution containing a surfactant and sodium cholate to form a dark-colored dispersion in water.[59] Overall, there is a clear trade-off between the transparency and conductivity of graphene films. The transmittance reported ranged from 35 to 90% with sheet resistances of $10^3$–$10^6\ \Omega\,sq^{-1}$. The thicker the film is, the lower the resistance is, but the poorer the transparency, and vice versa. Gee et al. demonstrated a simple method to synthesize high-quality, low-cost graphene in a large quantity by an electrochemical exfoliation process with artificial graphite as the starting material (Figure 12a,b). The TEs made of electrochemically exfoliated graphene can be simply prepared by an airbrush spraying method, which is easy to scale up for large-area deposition and compatible with flexible substrates.[60]

Another potential solution to the impasse of producing graphene on a large scale is to synthesize graphite oxide (GO) sheets. The GO can be reduced to graphene afterwards.[61] GO is usually made by oxidizing graphite with strong acids, followed by intercalation and exfoliation in water. The formation of GO has enabled chemists to safely manipulate GO sheets in water through a wide range of processes. The downside of this approach is postreduction. In some areas on the GO sheets, the $sp^2$ carbon networks seem to be irreversibly destroyed to give pockets of $sp^3$ carbon centers that act as electron traps. Soluble single-layered GO inks were assembled into high-quality patterns by printing on diverse flexible substrates, including paper, poly(ethylene terephthalate) (PET), and polyimide by a simple, low-cost ink-jet printing technique (Figure 12c). This method has great potential for the fabrication of flexible, low-cost TEs.[62]

Zhi and co-workers reported a novel strategy to produce uniformly reduced GO films on a large scale directly on PET substrates by using a rod-coating technique.[63] Meyer rod coating is a well-known technique that is widely used for making films in a continuous and controlled manner. This technique can be used in a scalable way for roll-to-roll production in industry (Figure 12d,e). Wang et al. used a dip-coating method to obtain uniform layers of GO on quartz surfaces.[64] The GO films were then thermally reduced in an oxygen-free environment to give a resistivity of 1.8 $k\Omega\,sq^{-1}$ at a transparency of over 70%. Additionally, they fabricated dye-sensitized SCs to demonstrate the utility of the printed films. The resulting PCE showed that the graphene-based cell was 30% less efficient than its ITO counterpart.

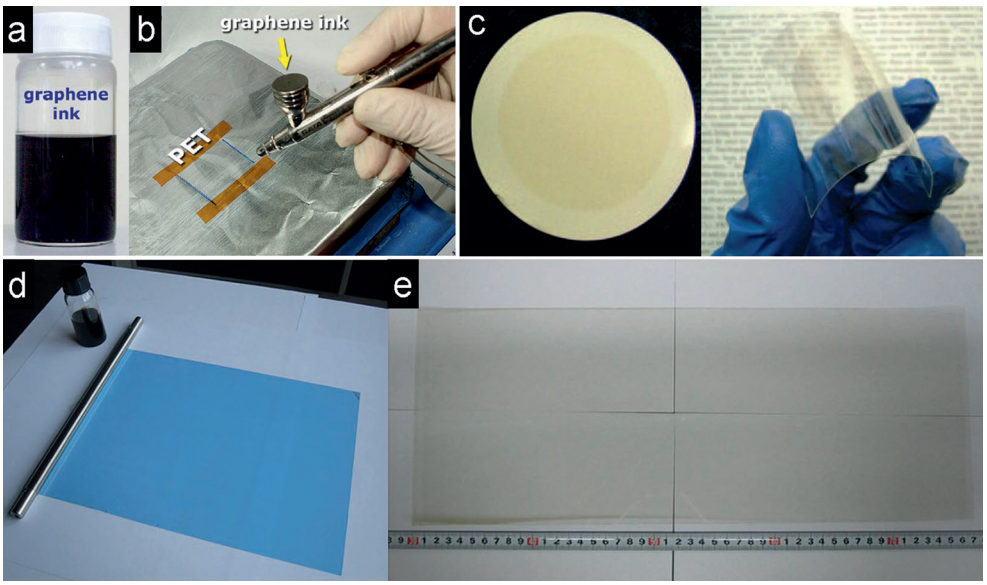


***Figure 12.*** Photographs showing a) an exfoliated-graphene ink and b) its deposition by the airbrush spraying method. c) Photographs of a GO film on a filtration membrane and a plastic substrate. d) Rod-coating setup for the fabrication of a GO film. e) Photograph of a large-scale GO film deposited on PET.

Wu et al. demonstrated the solution processing of GO by the Hummers method and its further reduction to graphene.[65] The graphene films (ca. 7 nm), with a sheet resistance of about 800 $\Omega\,sq^{-1}$ and 82% transmission at 550 nm, were used as TEs for OLEDs. These values are lower than the theoretical values owing to the existence of multiple grain boundaries, lattice defects, and oxidative traps formed during the fabrication process. OLEDs with a solution-processed graphene electrode showed a turn-on voltage of 4.5 V and a luminance of 300 $cd\,m^{-2}$ at 11.7 V; these properties are comparable to those of ITO-based OLEDs, which have a turn-on voltage of 3.8 V and a luminance of 300 $cd\,m^{-2}$ at 9.9 V.

### 2.4. Carbon-Nanotube Inks

Recent advances in solution-processed materials have enabled the development of several alternatives to sputtered ITO. The ability to apply nanomaterials from the liquid phase opens the possibility of printing these electronic materials and thus greatly increasing yield and throughput at a low cost, whereas the nanomaterial topology enables the creation of truly flexible devices. Carbon nanotubes (CNTs), tubular carbon-based nanostructures that can be envisaged as graphene rolled up into seamless cylinders, are ideal candidates for use in flexible electronics owing to their unique properties, such as their high intrinsic carrier mobility, conductivity, and mechanical flexibility. Therefore, random CNT networks are widely applied in optoelectronics. Furthermore, the high stability, flexibility, and mobility make CNT networks potential candidates for the replacement of rigid ITO.[66] CNTs are ideal for the construction of TEs owing to their high intrinsic conductivity, suitability for solution processing, flexibility, and potential for production at a low cost.[67]

Despite their intrinsic tendency to aggregate, CNTs can be dispersed well in solution in a similar way to "inks" upon chemical modification or the use of solubilizing additives, such as surfactants, cellulose derivatives, or conducting polymers, and can then be used to print electrodes through existing solution-based printing processes. The printing of CNTs has several advantages, such as enabling lower capital-equipment costs, higher throughput, and additive patterning.[68] Figure 13 shows photographs of several vials of CNT ink and films printed with CNTs that were fabricated by a slot-die and roll-to-roll process.[68a]

The excellent mechanical properties of CNTs enable potential applications in future flexible and stretchable optoelectronic devices.[68c,69] The CNT TEs synthesized by Hu et al. sustained up to 700% strain when uniaxially stretched.[70] No other reported film has maintained good conductivity when stretched to this extent. Fukushima and co-workers developed transparent, conducting CNT films on a PDMS substrate that can be rendered stretchable by applying strain along an axis and then releasing this strain. This process produced films that accommodated strains of up to 150% and demonstrated a conductivity as high as 2200 $S\,cm^{-1}$ in the stretched state: the most conductive stretchable CNT films reported to date.[68b,71] Transferred CNT films with a thickness of 20 nm exhibited excellent performance with a sheet resistance of 223 $\Omega\,sq^{-1}$ and a transparency of 90% at 550 nm. Most importantly, the as-prepared free-standing CNT films with a thickness of 20 nm showed extremely high tensile strength up to 850 MPa, which has great significance for practical applications of TEs.[69d]

Stretchable OLEDs based on CNT networks as the TEs were also built. The electroluminescence (EL) efficiency of the devices could be sustained under 45% strain, which is not possible for traditional ITO.[72] The device with the CNT electrode had a comparable lifetime to that of ITO. The acid resistance of the CNT electrode to poly(3,4-ethylenedioxythiophene) polystyrene sulfonate (PEDOT:PSS) was better than that of ITO after long-term operation. The application of transparent, conductive CNT networks as TEs in flexible OLEDs was investigated.[73] In comprehensive studies in which these networks were compared with commonly used ITO, CNT networks demonstrated excellent optical and superior mechanical properties. CNT networks exhibited more durable electrical properties under bending when used in OLEDs. The devices showed outstanding light output as well as a comparable lifetime performance to that of ITO-based devices, and could meet display requirements.

To enhance the performance of OLEDs, a method involving PEDOT passivation for better surface smoothness and $SOCl_2$ doping for lower sheet resistance was proposed. The optimized films showed a typical sheet resistance of approximately 160 $\Omega\,sq^{-1}$ at 87% transparency and were used successfully to make OLEDs with high stability and long lifetimes.[74] Pei and co-workers reported the fabrication of fully solution processed PLEDs by spin coating, rod coating, and/or blade coating. The all-solution-based device, which can be fabricated with high throughput, exhibited good flexibility and uniform light emission. The device showed better performance than conventional devices fabricated on a ITO anode with evaporated Al as the cathode.[75]

Rowell et al. studied the use of CNT films as anodes in flexible bulk-heterojunction (BHT) OSCs. The CNT inks were vacuum filtered and transferred onto a PET substrate. The films were then spin coated with PEDOT:PSS to reduce their roughness. The devices were shown to be much more flexible than the traditionally used ITO devices and had a PCE of 2.5%.[76] The aligned and uniform dispersion of CNTs in the PEDOT:PSS matrix favors electron conduction and can promote the rearrangement of PEDOT chains into a more extended conformation through π–π interactions. The CNT electrodes exhibited high conductivity of 3264.27 $S\,cm^{-1}$ with a high transmittance of over 85%, and the corresponding

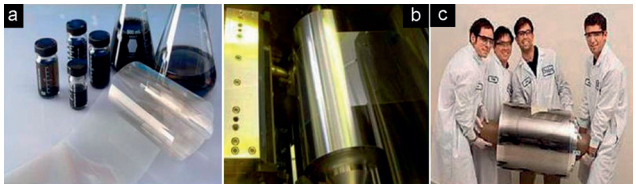


***Figure 13.*** Photographs showing a) vials of CNT inks, b) a CNT conductive film being coated by a slot die, and c) a roll of printed transparent conducting film of CNTs on PET.

ITO-free OSCs showed a PCE of 7.47% with high stability. Furthermore, a large-scale flexible electrode with excellent properties was obtained by a roll-to-roll technique (Figure 14). A combination of the flexible and conductive CNT film with the scalable roll-to-roll process is expected to enable the commercial production of large-scale TEs that can replace ITO in the near future.[77]

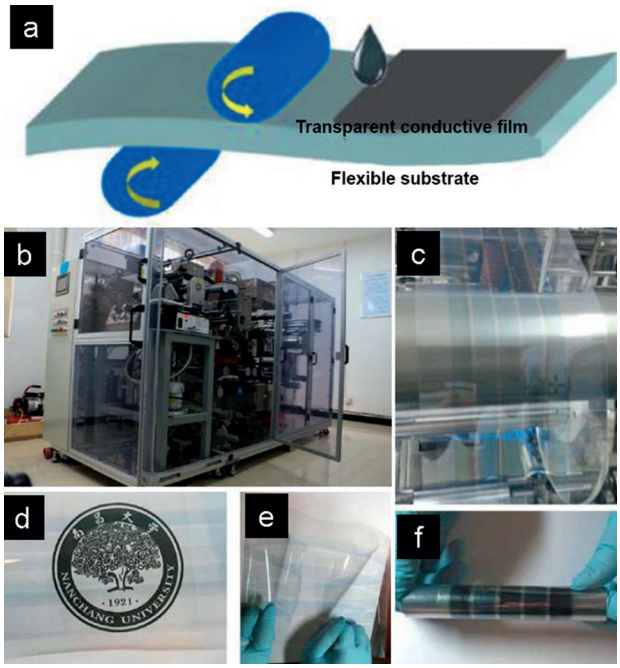


***Figure 14.*** a) Schematic illustration of and b) machine used for the roll-to-roll process. c–f) Photographs of gravure-printed TEs with superior flexibility and transparency, and a sheet resistance of 17 $\Omega sq^{-1}$.

Transparent and flexible ZnO-nanowire UV PDs, in which CNT thin films were used as TEs, were prepared by a solution-based method.[78] The CNT films were obtained by a filtration method and then transferred onto flexible substrates for ZnO NW growth. The photoresponse current of the PDs was found to be in proportion to the ZnO NW density. The density could be tuned to increase the photocurrent by a factor of 300. The decay time for the fabricated PDs was found to be as low as 16 s. This study suggested the possibility of fabricating inexpensive, visible-blind UV PDs by solution-based methods. Faclo et al. demonstrated fully sprayed organic photodiodes on PET substrates.[79] CNT TEs with a sheet resistance of 160 $\Omega sq^{-1}$ at 84% transmittance were spray deposited from ink solutions. Subsequently, a PEDOT:PSS layer and a blend of poly(3-hexylthiophen-2,5-diyl) (P3HT) and phenyl-$C_{61}$-butyric acid methyl ester (PCBM) were deposited by spray printing. The optimized device achieved a yield above 90% with a dark current as low as $10^{-4}$ $mA cm^{-2}$ and an external quantum efficiency of 65% with high reproducibility.

### *2.5. Hybrid Inks and Assembled TEs*

The performance of simple NC-ink-based TEs has not reached the standard required for commercial applications. For example, the electrical properties of the TCO NC films is not optimal for optoelectronics. The surface roughness of the metal NW films has restricted their practical application. In the case of the CNT films, although the smaller CNT bundles lead to higher conductivity, the inner tubes within the bundle may be partially shielded from electrical contact with the overall network, thus prohibiting their participation in the current-carrying capacity of the network. The largest source of resistance in a macroscopic film arises from the intersections between CNT bundles. Recent reports suggest that the solution processing of hybrid films[80] is a promising concept for the development of transparent conducting technologies.

Hybrid CNT/Ag nanocomposites combine the enhanced mechanical compliance, electrical performance, and optical transparency of small CNTs with the enhanced electrical conductivity of a Ag NW backbone. The composites have efficient electron-transport paths with NWs as a backbone current collector and a local CNT percolation network.[81]

Films composed of graphene and random networks of metal NWs[82] also exhibited impressive stability under mechanical bending. The development of such high-performance hybrid structures provides a route towards robust, scalable, and low-cost approaches to practical TEs. Hybrid TEs composed of graphene and a network of 1D metal NWs exhibited a low sheet resistance (33 $\Omega sq^{-1}$) at a high transmittance (94%), robust stability against electrical breakdown and oxidation, and superb flexibility (27% bending strain) and stretchability (100% tensile strain). These multiple functionalities of hybrid structures suggest the future potential of next-generation TEs.[83]

A two-dimensional GO nanosheet is transparent, highly dispersible in water, and hydrophilic, and is thus ideal for use as a coating and protective layer for metal-nanowire-based TEs. As such ultrathin 2D adhesive GO nanosheets were expected to tightly hold Ag NWs to reduce the sheet resistance and produce a uniform film surface, large-area, flexible, and highly transparent Ag NW/GO TEs were prepared.[84] The hybrid film was fabricated by a two-step procedure: bar or spray coating of an Ag NW ink onto a PET substrate, followed by spray coating of the GO ink (Figure 15). The novel TEs exhibited superior properties, including a low sheet resistance of 24.8 $\Omega sq^{-1}$ and high durability (over 10000 cycles at a bending radius of 2 mm), good chemical and adhesive stability, and a high transparency of 92% at 550 nm.

The key issues associated with the fabrication of high-quality NW electrodes are the maintenance of their electrical properties under harsh chemical and mechanical conditions, and their preparation with a smoother surface morphology. The introduction of a metal-oxide buffer layer to enhance the stability and surface smoothness of the NW electrodes is a promising concept.[50b,85] The wrapping of Ag NWs with conductive ITO NCs reduces wire-to-wire junction resistance and leads to a smooth surface morphology and excellent mechanical adhesion and flexibility while maintaining high

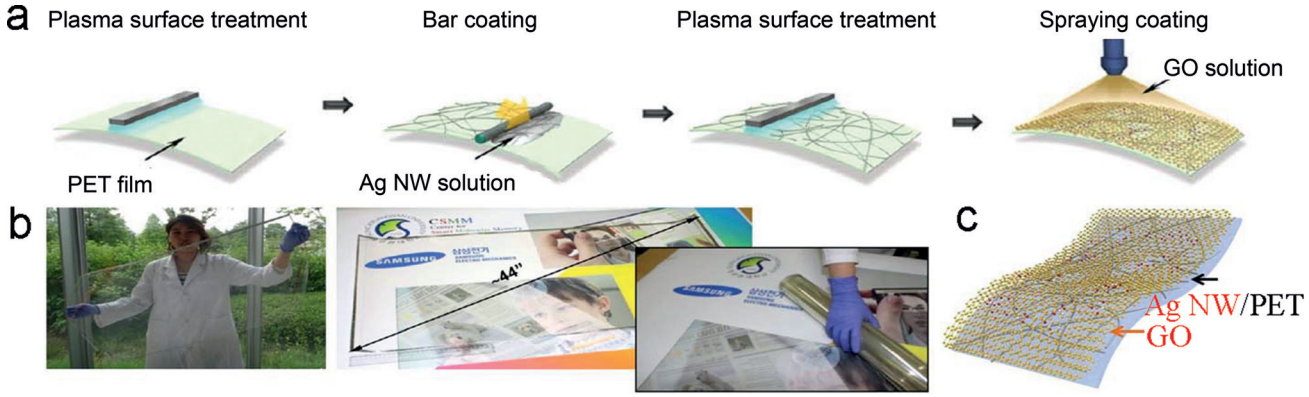


***Figure 15.*** a) Schematic illustration of the fabrication of a GO/Ag NW/PET film. b) Photographs of the flexible TE produced by spray coating. c) Schematic structure of the flexible GO/Ag NW/PET film.

transmittance and low sheet resistance. The transmittance of hybrid TEs at 550 nm reached 90.5% when the sheet resistance was 44 $\Omega\,sq^{-1}$. Various metal-nanowire meshes embedded in various conductive NCs matrices can serve effectively as hybrid TEs for a wide variety of optoelectronic devices owing to their superior performance and simple, cost-effective, and gentle processing.[86]

TEs based on Ag NW percolation networks modified with GO were also prepared. The monatomic thickness, mechanical flexibility, and strong bonding with Ag NWs enable the GO sheets to wrap around and solder the NW junctions to dramatically reduce the inter-nanowire contact resistance without heat treatment or high-force pressing. The GO-soldered Ag NW network processed from inks had a figure-of-merit sheet resistance of 14 $\Omega\,sq^{-1}$ with 88% transmittance at 550 nm. Its storage stability was improved as compared to that of a conventional Ag NW network annealed at high temperature. When bent at a 4 mm bending radius, its sheet resistance was increased by only 2–3% after 12000 bending cycles. Composite TEs fabricated by inlaying a GO-soldered Ag NW network in the surface layer of polymer films were stretchable under a 100% linear strain without a decrease in the electrical conductivity. Fully stretchable white PLEDs were fabricated with the stretchable TEs. The PLEDs survived 100 stretching cycles between 0 and 40% strain and could be stretched up to a 130% linear strain.[87]

Large-area graphene films were prepared by the spray coating of a hybrid ink of electrochemically exfoliated graphene and a commercially available PEDOT:PSS formulation (Clevios PH1000) in DMF. The thickness of the conductive graphene films, with a conductivity of approximately 1000 $S\,cm^{-1}$ and a transmittance of 80% at 500 nm, can be tailored from 10 to 20 nm by the spray-coating method. An ultrathin PD device based on a P3HT:PCBM blend as the photoactive layer was fabricated by employing the as-obtained hybrid TEs. The device had a thickness of about 3 μm, including the substrate, and exhibited excellent performance with a detectivity of $1.33\times10^{12}$ jones at 500 nm, which compares well with that of state-of-the-art silicon-based PDs.[88]

## 3. Outlook

ITO has been the most widely used material for TEs for decades, and is likely to continue to play that role well into the future. However, the expense and low utilization rate of the targets, the harsh vacuum-deposition conditions, and the intrinsic brittleness of ITO hinder its application in many smart optoelectronic devices. The replacement of traditional doped metal oxides (mainly ITO) used for TEs with novel NCs could make a revolutionary impact on modern optoelectronics. The development of low-cost, flexible, stretchable TEs is imperative for novel applications. TEs assembled from NC inks exhibit huge potential for practical applications in various smart optoelectronic devices. The NC inks are inexpensive, and facile solution-based printing techniques can be used to generate large-area and patterned films. Films assembled from NC inks are receiving increasing attention as next-generation TEs for optoelectronic devices.

NCs developed for use as inks mainly include TCOs, metal NWs, CNTs, and graphene. In spite of the remarkable scientific progress in the synthesis and application of NCs, these inks will require considerable further development before they can be used in real applications in industry. It is imperative to explore appropriate ways to further improve the electrical conductivity of TCO NCs for their use in high-performance devices. A broad range of applications can be envisaged for metal NWs with high conductivity and mechanical flexibility. Several investigations have shown that metal-nanowire networks enable new technologies, such as flexible SCs, heaters, touch screens, and stretchable electronics. Issues that need to be addressed for certain applications are the environmental stability, high surface roughness, and success ratio of metal NWs in the resulting devices. CNT and graphene inks have become popular components of optoelectronic devices as TEs. As CNT doping, separation, and synthesis continue to improve, device-integration issues are still waiting to be solved. Graphene films are currently in a far earlier stage of development, and questions remain regarding the ultimate conductivity that can be achieved with straightforward manufacturing techniques. However, graphene should be superior to CNTs in terms of surface roughness.

Furthermore, the combination of several types of NC inks could lead to highly efficient hybrid TEs with superior properties.

Given the progress made to date, TEs assembled from NC inks show promise for next-generation printable, flexible devices and could make a revolutionary impact on modern optoelectronics. As the existing synthetic methods are becoming mature, future research should also focus on the development of novel process technologies that were previously inconceivable. The advantages of NC inks include the potential of scaling up the fabrication process to enable mass production and the relatively low materials and manufacturing costs, which are especially appealing for next-generation flexible electrodes and printable substrates. One of the biggest problems is the device-integration issue, which must be solved. This field is at a very early stage of research and development, but it offers extremely promising prospects and application opportunities in smart optoelectronics.

## Acknowledgements

This work was financially supported by the National Basic Research Program of China (2014CB931700/2014CB931702), the NSFC (61222403), and the Priority Academic Program Development of Jiangsu Higher Education Institutions (PAPD).

**How to cite:** *Angew. Chem. Int. Ed.* **2015**, *54*, 9760–9774
*Angew. Chem.* **2015**, *127*, 9896–9910

[1] a) J. Cui, A. Wang, N. L. Edleman, J. Ni, P. Lee, N. R. Armstrong, T. J. Marks, *Adv. Mater.* **2001**, *13*, 1476–1480; b) D. S. Hecht, L. Hu, G. Irvin, *Adv. Mater.* **2011**, *23*, 1482–1513; c) P. D. C. King, T. D. Veal, *J. Phys. Condens. Matter* **2011**, *23*, 334214; d) D. S. Ginley, C. Bright, *MRS Bull.* **2000**, *25*, 15–18.

[2] a) H. Kim, J. S. Horwitz, S. B. Qadri, D. B. Chrisey, *Thin Solid Films* **2002**, *420*, 107–111; b) J.-H. Kim, H. Lee, S. Choi, K. H. Bae, J. Y. Park, *Thin Solid Films* **2013**, *547*, 163–167.

[3] a) H. Hong, H. Jung, S.-J. Hong, *Res. Chem. Intermed.* **2010**, *36*, 761–766; b) J. Musil, J. Vlček, *Surf. Coat. Technol.* **1999**, *112*, 162–169.

[4] a) F. Xu, Y. Zhu, *Adv. Mater.* **2012**, *24*, 5117–5122; b) J. Lewis, S. Grego, B. Chalamala, E. Vick, D. Temple, *Appl. Phys. Lett.* **2004**, *85*, 3450–3452.

[5] a) H. Wu, D. S. Kong, Z. C. Ruan, P. C. Hsu, S. Wang, Z. F. Yu, T. J. Carney, L. B. Hu, S. H. Fan, Y. Cui, *Nat. Nanotechnol.* **2013**, *8*, 421–425; b) S. Brovelli, N. Chiodini, R. Lorenzi, A. Lauria, M. Romagnoli, A. Paleari, *Nat. Commun.* **2012**, *3*, 690; c) J. Song, S. A. Kulinich, J. Yan, Z. Li, J. He, C. Kan, H. Zeng, *Adv. Mater.* **2013**, *25*, 5750–5755.

[6] A. Kumar, C. Zhou, *ACS Nano* **2010**, *4*, 11–14.

[7] D. Lee, D. Paeng, H. K. Park, C. P. Grigoropoulos, *ACS Nano* **2014**, *8*, 9807–9814.

[8] a) K.-W. Park, S.-B. Kang, J.-A. Jeong, S.-W. Choi, J. Kim, I.-K. You, Y. S. Yang, H.-K. Kim, *J. Phys. D* **2013**, *46*, 145301; b) J. Kim, S. I. Na, H. K. Kim, *Sol. Energy Mater. Sol. Cells* **2012**, *98*, 424–432.

[9] a) J.-A. Jeong, J. Lee, H. Kim, H.-K. Kim, S.-I. Na, *Sol. Energy Mater. Sol. Cells* **2010**, *94*, 1840–1844; b) H. K. Kim, I. K. You, J. B. Koo, S. H. Kim, *Surf. Coat. Technol.* **2012**, *211*, 33–36.

[10] a) J. A. Jeong, Y. J. Jeon, S. S. Kim, B. K. Kim, K. B. Chung, H. K. Kim, *Sol. Energy Mater. Sol. Cells* **2014**, *122*, 241–250; b) H.-M. Lee, J.-A. Jeong, S.-W. Choi, J. Kim, H.-K. Kim, *J. Sol-Gel Sci. Technol.* **2015**, *73*, 531–535.

[11] D. A. Alsaid, E. Rebrosova, M. Joyce, M. Rebros, M. Atashbar, B. Bazuin, *J. Disp. Technol.* **2012**, *8*, 391–396.

[12] G. Bühler, D. Tholmann, C. Feldmann, *Adv. Mater.* **2007**, *19*, 2224–2227.

[13] R. Buonsanti, A. Llordes, S. Aloni, B. A. Helms, D. J. Milliron, *Nano Lett.* **2011**, *11*, 4706–4710.

[14] J. Lee, S. Lee, G. Li, M. A. Petruska, D. C. Paine, S. Sun, *J. Am. Chem. Soc.* **2012**, *134*, 13410–13414.

[15] B. T. Diroll, T. R. Gordon, E. A. Gaulding, D. R. Klein, T. Paik, H. J. Yun, E. D. Goodwin, D. Damodhar, C. R. Kagan, C. B. Murray, *Chem. Mater.* **2014**, *26*, 4579–4588.

[16] D. Ito, S. Yokoyama, T. Zaikova, K. Masuko, J. E. Hutchison, *ACS Nano* **2014**, *8*, 64–75.

[17] X. Liu, M. T. Swihart, *Nanoscale* **2013**, *5*, 8029–8036.

[18] J. Song, S. A. Kulinich, J. Li, Y. Liu, H. Zeng, *Angew. Chem. Int. Ed.* **2015**, *54*, 462–466; *Angew. Chem.* **2015**, *127*, 472–476.

[19] E. Della Gaspera, A. S. R. Chesman, J. van Embden, J. J. Jasieniak, *ACS Nano* **2014**, *8*, 9154–9163.

[20] L. Luo, D. Bozyigit, V. Wood, M. Niederberger, *Chem. Mater.* **2013**, *25*, 4901–4907.

[21] E. Della Gaspera, M. Bersani, M. Cittadini, M. Guglielmi, D. Pagani, R. Noriega, S. Mehra, A. Salleo, A. Martucci, *J. Am. Chem. Soc.* **2013**, *135*, 3439–3448.

[22] J. Lee, M. A. Petruska, S. Sun, *J. Phys. Chem. C* **2014**, *118*, 12017–12021.

[23] a) Y. Cheng, S. Wang, R. Wang, J. Sun, L. Gao, *J. Mater. Chem. C* **2014**, *2*, 5309–5316; b) B. Han, K. Pei, Y. Huang, X. Zhang, Q. Rong, Q. Lin, Y. Guo, T. Sun, C. Guo, D. Carnahan, M. Giersig, Y. Wang, J. Gao, Z. Ren, K. Kempa, *Adv. Mater.* **2014**, *26*, 873–877; c) M.-G. Kang, H. J. Park, S. H. Ahn, L. J. Guo, *Sol. Energy Mater. Sol. Cells* **2010**, *94*, 1179–1184; d) Y. Yu, C. Yan, Z. Zheng, *Adv. Mater.* **2014**, *26*, 5508–5516; e) P.-C. Hsu, D. Kong, S. Wang, H. Wang, A. J. Welch, H. Wu, Y. Cui, *J. Am. Chem. Soc.* **2014**, *136*, 10593–10596; f) J. Yeo, S. Hong, D. Lee, N. Hotz, M.-T. Lee, C. P. Grigoropoulos, S. H. Ko, *Plos One* **2012**, *7*, e42315.

[24] a) J. Ge, H. B. Yao, X. Wang, Y. D. Ye, J. L. Wang, Z. Y. Wu, J. W. Liu, F. J. Fan, H. L. Gao, C. L. Zhang, S. H. Yu, *Angew. Chem. Int. Ed.* **2013**, *52*, 1654–1659; *Angew. Chem.* **2013**, *125*, 1698–1703; b) H. Y. Jang, S.-K. Lee, S. H. Cho, J.-H. Ahn, S. Park, *Chem. Mater.* **2013**, *25*, 3535–3538; c) A. Sánchez-Iglesias, B. Rivas-Murias, M. Grzelczak, J. Pérez-Juste, L. M. Liz-Marzán, F. Rivadulla, M. A. Correa-Duarte, *Nano Lett.* **2012**, *12*, 6066–6070; d) H. Wu, M. Menon, E. Gates, A. Balasubramanian, C. J. Bettinger, *Adv. Mater.* **2014**, *26*, 706–711.

[25] a) T. Kim, A. Canlier, G. H. Kim, J. Choi, M. Park, S. M. Han, *ACS Appl. Mater. Interfaces* **2013**, *5*, 788–794; b) L. Yang, T. Zhang, H. Zhou, S. C. Price, B. J. Wiley, W. You, *ACS Appl. Mater. Interfaces* **2011**, *3*, 4075–4084; c) T. C. Hauger, S. M. I. Al-Rafia, J. M. Buriak, *ACS Appl. Mater. Interfaces* **2013**, *5*, 12663–12671; d) A. R. Madaria, A. Kumar, C. Zhou, *Nanotechnology* **2011**, *22*, 245201.

[26] a) J.-W. Lim, D.-Y. Cho, K. Eun, S.-H. Choa, S.-I. Na, J. Kim, H.-K. Kim, *Sol. Energy Mater. Sol. Cells* **2012**, *105*, 69–76; b) D. Langley, G. Giusti, C. Mayousse, C. Celle, D. Bellet, J.-P. Simonato, *Nanotechnology* **2013**, *24*, 452001; c) H.-F. Cui, Y.-F. Zhang, C.-N. Li, *Opt. Eng.* **2014**, *53*, 077102–077102.

[27] S. Nam, M. Song, D.-H. Kim, B. Cho, H. M. Lee, J.-D. Kwon, S.-G. Park, K.-S. Nam, Y. Jeong, S.-H. Kwon, Y. C. Park, S.-H. Jin, J.-W. Kang, S. Jo, C. S. Kim, *Sci. Rep.* **2014**, *4*, 4788.

[28] a) A. R. Madaria, A. Kumar, F. N. Ishikawa, C. Zhou, *Nano Res.* **2010**, *3*, 564–573; b) P. Lee, J. Lee, H. Lee, J. Yeo, S. Hong, K. H. Nam, D. Lee, S. S. Lee, S. H. Ko, *Adv. Mater.* **2012**, *24*, 3326–3332.

[29] a) L. Hu, H. S. Kim, J.-Y. Lee, P. Peumans, Y. Cui, *ACS Nano* **2010**, *4*, 2955–2963; b) S. Kiruthika, R. Gupta, K. D. M. Rao, S.

  

Chakraborty, N. Padmavathy, G. U. Kulkarni, *J. Mater. Chem. C* **2014**, *2*, 2089 – 2094.
[30] a) Y. G. Sun, B. Gates, B. Mayers, Y. N. Xia, *Nano Lett.* **2002**, *2*, 165 – 168; b) Y. G. Sun, Y. N. Xia, *Adv. Mater.* **2002**, *14*, 833 – 837; c) J. Lee, I. Lee, T.-S. Kim, J.-Y. Lee, *Small* **2013**, *9*, 2887 – 2894.
[31] T. Akter, W. S. Kim, *ACS Appl. Mater. Interfaces* **2012**, *4*, 1855 – 1859.
[32] H. Lee, K. Lee, J. T. Park, W. C. Kim, H. Lee, *Adv. Funct. Mater.* **2014**, *24*, 3276 – 3283.
[33] D. Angmo, M. Hosel, F. C. Krebs, *Sol. Energy Mater. Sol. Cells* **2012**, *107*, 329 – 336.
[34] a) L. Zhou, H.-Y. Xiang, S. Shen, Y.-Q. Li, J.-D. Chen, H.-J. Xie, I. A. Goldthorpe, L.-S. Chen, S.-T. Lee, J.-X. Tang, *ACS Nano* **2014**, *8*, 12796 – 12805; b) T. B. Song, Y. Chen, C. H. Chung, Y. Yang, B. Bob, H. S. Duan, G. Li, K. N. Tu, Y. Huang, Y. Yang, *ACS Nano* **2014**, *8*, 2804 – 2811.
[35] a) B. Aksoy, S. Coskun, S. Kucukyildiz, H. E. Unalan, *Nanotechnology* **2012**, *23*, 325202; b) J. Wang, C. Yan, W. Kang, P. S. Lee, *Nanoscale* **2014**, *6*, 10734 – 10739.
[36] S.-B. Kang, Y.-J. Noh, S.-I. Na, H.-K. Kim, *Sol. Energy Mater. Sol. Cells* **2014**, *122*, 152 – 157.
[37] M. Song, D. S. You, K. Lim, S. Park, S. Jung, C. S. Kim, D.-H. Kim, D.-G. Kim, J.-K. Kim, J. Park, Y.-C. Kang, J. Heo, S.-H. Jin, J. H. Park, J.-W. Kang, *Adv. Funct. Mater.* **2013**, *23*, 4177 – 4184.
[38] F. Guo, P. Kubis, N. Li, T. Przybilla, G. Matt, T. Stubhan, T. Ameri, B. Butz, E. Spiecker, K. Forberich, C. J. Brabec, *ACS Nano* **2014**, *8*, 12632 – 12640.
[39] a) L. Li, Z. Yu, W. Hu, C.-h. Chang, Q. Chen, Q. Pei, *Adv. Mater.* **2011**, *23*, 5563 – 5567; b) M. Amjadi, A. Pichitpajongkit, S. Lee, S. Ryu, I. Park, *ACS Nano* **2014**, *8*, 5154 – 5163; c) C. K. Gong, J. J. Liang, W. Hu, X. F. Niu, S. W. Ma, H. T. Hahn, Q. B. Pei, *Adv. Mater.* **2013**, *25*, 4186 – 4191; d) J. Li, J. Liang, L. Li, F. Ren, W. Hu, J. Li, S. Qi, Q. Pei, *ACS Nano* **2014**, *8*, 12874 – 12882; e) W. Hu, X. Niu, R. Zhao, Q. Pei, *Appl. Phys. Lett.* **2013**, *102*, 083303.
[40] Z. B. Yu, Q. W. Zhang, L. Li, Q. Chen, X. F. Niu, J. Liu, Q. B. Pei, *Adv. Mater.* **2011**, *23*, 664 – 668.
[41] W. Gaynor, S. Hofmann, M. G. Christoforo, C. Sachse, S. Mehra, A. Salleo, M. D. McGehee, M. C. Gather, B. Lüssem, L. Müller-Meskamp, P. Peumans, K. Leo, *Adv. Mater.* **2013**, *25*, 4006 – 4013.
[42] J. J. Liang, L. Li, X. F. Niu, Z. B. Yu, Q. B. Pei, *Nat. Photonics* **2013**, *7*, 817 – 824.
[43] C. Y. Yan, J. X. Wang, X. Wang, W. B. Kang, M. Q. Cui, C. Y. Foo, P. S. Lee, *Adv. Mater.* **2014**, *26*, 943 – 950.
[44] J. Wang, C. Yan, M.-F. Lin, K. Tsukagoshi, P. S. Lee, *J. Mater. Chem. C* **2015**, *3*, 596 – 600.
[45] a) A. R. Rathmell, B. J. Wiley, *Adv. Mater.* **2011**, *23*, 4798 – 4803; b) H. J. Yang, S. Y. He, H. Y. Tuan, *Langmuir* **2014**, *30*, 602 – 610; c) D. Q. Zhang, R. R. Wang, M. C. Wen, D. Weng, X. Cui, J. Sun, H. X. Li, Y. F. Lu, *J. Am. Chem. Soc.* **2012**, *134*, 14283 – 14286; d) Y. Tang, S. Gong, Y. Chen, L. W. Yap, W. L. Cheng, *ACS Nano* **2014**, *8*, 5707 – 5714; e) I. E. Stewart, A. R. Rathmell, L. Yan, S. R. Ye, P. F. Flowers, W. You, B. J. Wiley, *Nanoscale* **2014**, *6*, 5980 – 5988; f) C. Sachse, N. Weiß, N. Gaponik, L. Müller-Meskamp, A. Eychmüller, K. Leo, *Adv. Energy Mater.* **2014**, *4*, 1300737.
[46] Y. Chang, M. L. Lye, H. C. Zeng, *Langmuir* **2005**, *21*, 3746 – 3748.
[47] A. R. Rathmell, S. M. Bergin, Y. L. Hua, Z. Y. Li, B. J. Wiley, *Adv. Mater.* **2010**, *22*, 3558 – 3563.
[48] a) S. J. Li, Y. Y. Chen, L. J. Huang, D. C. Pan, *Inorg. Chem.* **2014**, *53*, 4440 – 4444; b) C. Mayousse, C. Celle, A. Carella, J. P. Simonato, *Nano Res.* **2014**, *7*, 315 – 324; c) H. Z. Guo, N. Lin, Y. Z. Chen, Z. W. Wang, Q. S. Xie, T. C. Zheng, N. Gao, S. P. Li, J. Y. Kang, D. J. Cai, D. L. Peng, *Sci. Rep.* **2013**, *3*, 2323.
[49] W. L. Hu, R. R. Wang, Y. F. Lu, Q. B. Pei, *J. Mater. Chem. C* **2014**, *2*, 1298 – 1305.
[50] a) A. R. Rathmell, N. Minh, M. Chi, B. J. Wiley, *Nano Lett.* **2012**, *12*, 3193 – 3199; b) Z. F. Chen, S. R. Ye, I. E. Stewart, B. J. Wiley, *ACS Nano* **2014**, *8*, 9673 – 9679; c) Y. Won, A. Kim, D. Lee, W. Yang, K. Woo, S. Jeong, J. Moon, *NPG Asia Mater.* **2014**, *6*, e105.
[51] J. Z. Song, J. H. Li, J. Y. Xu, H. B. Zeng, *Nano Lett.* **2014**, *14*, 6298 – 6305.
[52] Y. Won, A. Kim, W. Yang, S. Jeong, J. Moon, *NPG Asia Mater.* **2014**, *6*, e132.
[53] S. Han, S. Hong, J. Ham, J. Yeo, J. Lee, B. Kang, P. Lee, J. Kwon, S. S. Lee, M.-Y. Yang, S. H. Ko, *Adv. Mater.* **2014**, *26*, 5808 – 5814.
[54] H. G. Im, S. H. Jung, J. Jin, D. Lee, J. Lee, D. Lee, J. Y. Lee, I. D. Kim, B. S. Bae, *ACS Nano* **2014**, *8*, 10973 – 10979.
[55] a) T. H. Han, Y. Lee, M. R. Choi, S. H. Woo, S. H. Bae, B. H. Hong, J. H. Ahn, T. W. Lee, *Nat. Photonics* **2012**, *6*, 105 – 110; b) J. K. Wassei, R. B. Kaner, *Mater. Today* **2010**, *13*, 52 – 59; c) N. O. Weiss, H. Zhou, L. Liao, Y. Liu, S. Jiang, Y. Huang, X. Duan, *Adv. Mater.* **2012**, *24*, 5782 – 5825.
[56] C. Soldano, A. Mahmood, E. Dujardin, *Carbon* **2010**, *48*, 2127 – 2150.
[57] a) X. L. Li, G. Y. Zhang, X. D. Bai, X. M. Sun, X. R. Wang, E. Wang, H. J. Dai, *Nat. Nanotechnol.* **2008**, *3*, 538 – 542; b) E. B. Secor, P. L. Prabhumirashi, K. Puntambekar, M. L. Geier, M. C. Hersam, *J. Phys. Chem. Lett.* **2013**, *4*, 1347 – 1351.
[58] P. Blake, P. D. Brimicombe, R. R. Nair, T. J. Booth, D. Jiang, F. Schedin, L. A. Ponomarenko, S. V. Morozov, H. F. Gleeson, E. W. Hill, A. K. Geim, K. S. Novoselov, *Nano Lett.* **2008**, *8*, 1704 – 1708.
[59] S. De, P. J. King, M. Lotya, A. O'Neill, E. M. Doherty, Y. Hernandez, G. S. Duesberg, J. N. Coleman, *Small* **2010**, *6*, 458 – 464.
[60] C.-M. Gee, C.-C. Tseng, F.-Y. Wu, H.-P. Chang, L.-J. Li, Y.-P. Hsieh, C.-T. Lin, J.-C. Chen, *Displays* **2013**, *34*, 315 – 319.
[61] a) Q. Zheng, Z. Li, J. Yang, J.-K. Kim, *Prog. Mater. Sci.* **2014**, *64*, 200 – 247; b) K. Min, T. H. Han, J. Kim, J. Jung, C. Jung, S. M. Hong, C. M. Koo, *J. Colloid Interface Sci.* **2012**, *383*, 36 – 42; c) C.-L. Lee, C.-H. Chen, C.-W. Chen, *Chem. Eng. J.* **2013**, *230*, 296 – 302.
[62] a) G. Eda, G. Fanchini, M. Chhowalla, *Nat. Nanotechnol.* **2008**, *3*, 270 – 274; b) L. Huang, Y. Huang, J. Liang, X. Wan, Y. Chen, *Nano Res.* **2011**, *4*, 675 – 684; c) H. A. Becerril, J. Mao, Z. Liu, R. M. Stoltenberg, Z. Bao, Y. Chen, *ACS Nano* **2008**, *2*, 463 – 470; d) J. Wu, H. A. Becerril, Z. Bao, Z. Liu, Y. Chen, P. Peumans, *Appl. Phys. Lett.* **2008**, *92*, 263302.
[63] J. Wang, M. Liang, Y. Fang, T. Qiu, J. Zhang, L. Zhi, *Adv. Mater.* **2012**, *24*, 2874 – 2878.
[64] X. Wang, L. J. Zhi, K. Mullen, *Nano Lett.* **2008**, *8*, 323 – 327.
[65] J. B. Wu, M. Agrawal, H. A. Becerril, Z. N. Bao, Z. F. Liu, Y. S. Chen, P. Peumans, *ACS Nano* **2010**, *4*, 43 – 48.
[66] a) L. Cai, J. Li, P. Luan, H. Dong, D. Zhao, Q. Zhang, X. Zhang, M. Tu, Q. Zeng, W. Zhou, S. Xie, *Adv. Funct. Mater.* **2012**, *22*, 5238 – 5244; b) R. P. Tortorich, J.-W. Choi, *Nanomaterials* **2013**, *3*, 453 – 468; c) S. Park, M. Vosguerichian, Z. Bao, *Nanoscale* **2013**, *5*, 1727 – 1752.
[67] a) H. Okimoto, T. Takenobu, K. Yanagi, Y. Miyata, H. Shimotani, H. Kataura, Y. Iwasa, *Adv. Mater.* **2010**, *22*, 3981 – 3986; b) O. S. Kwon, H. Kim, H. Ko, J. Lee, B. Lee, C. H. Jung, J. H. Choi, K. Shin, *Carbon* **2013**, *58*, 116 – 127; c) C. Wang, D. Hwang, Z. B. Yu, K. Takei, J. Park, T. Chen, B. W. Ma, A. Javey, *Nat. Mater.* **2013**, *12*, 899 – 904; d) G. Schwartz, B. C. K. Tee, J. Mei, A. L. Appleton, D. H. Kim, H. Wang, Z. Bao, *Nat. Commun.* **2013**, *4*, 1859.
[68] a) D. S. Hecht, R. B. Kaner, *Mrs Bull.* **2011**, *36*, 749 – 755; b) T. Sekitani, Y. Noguchi, K. Hata, T. Fukushima, T. Aida, T. Someya, *Science* **2008**, *321*, 1468 – 1472; c) T. Sekitani, H. Nakajima, H. Maeda, T. Fukushima, T. Aida, K. Hata, T. Someya, *Nat. Mater.* **2009**, *8*, 494 – 499.

[69] a) S. Park, H. Kim, M. Vosgueritchian, S. Cheon, H. Kim, J. H. Koo, T. R. Kim, S. Lee, G. Schwartz, H. Chang, Z. A. Bao, *Adv. Mater.* **2014**, *26*, 7324 – 7332; b) S. Shian, R. M. Diebold, A. McNamara, D. R. Clarke, *Appl. Phys. Lett.* **2012**, *101*, 061101; c) J. Li, L. Hu, L. Wang, Y. Zhou, G. Gruner, T. J. Marks, *Nano Lett.* **2006**, *6*, 2472 – 2477; d) Z. Shi, X. Chen, X. Wang, T. Zhang, J. Jin, *Adv. Funct. Mater.* **2011**, *21*, 4358 – 4363.

[70] L. Hu, W. Yuan, P. Brochu, G. Gruner, Q. Pei, *Appl. Phys. Lett.* **2009**, *94*, 161108.

[71] a) D. J. Lipomi, M. Vosgueritchian, B. C.-K. Tee, S. L. Hellstrom, J. A. Lee, C. H. Fox, Z. N. Bao, *Nat. Nanotechnol.* **2011**, *6*, 788 – 792; b) Y. Zhu, F. Xu, *Adv. Mater.* **2012**, *24*, 1073 – 1077; c) T. Yamada, Y. Hayamizu, Y. Yamamoto, Y. Yomogida, A. Izadi-Najafabadi, D. N. Futaba, K. Hata, *Nat. Nanotechnol.* **2011**, *6*, 296 – 301.

[72] Z. B. Yu, X. F. Niu, Z. T. Liu, Q. B. Pei, *Adv. Mater.* **2011**, *23*, 3989 – 3994.

[73] L. Hu, J. Li, J. Liu, G. Grüner, T. Marks, *Nanotechnology* **2010**, *21*, 155202.

[74] D. H. Zhang, K. Ryu, X. L. Liu, E. Polikarpov, J. Ly, M. E. Tompson, C. W. Zhou, *Nano Lett.* **2006**, *6*, 1880 – 1886.

[75] J. Liang, L. Li, X. Niu, Z. Yu, Q. Pei, *J. Phys. Chem. C* **2013**, *117*, 16632 – 16639.

[76] M. W. Rowell, M. A. Topinka, M. D. McGehee, H.-J. Prall, G. Dennler, N. S. Sariciftci, L. Hu, G. Gruner, *Appl. Phys. Lett.* **2006**, *88*, 233506.

[77] X. Hu, L. Chen, Y. Zhang, Q. Hu, J. Yang, Y. Chen, *Chem. Mater.* **2014**, *26*, 6293 – 6302.

[78] E. S. Ates, S. Kucukyildiz, H. E. Unalan, *ACS Appl. Mater. Interfaces* **2012**, *4*, 5142 – 5146.

[79] A. Falco, L. Cina, G. Scarpa, P. Lugli, A. Abdellah, *ACS Appl. Mater. Interfaces* **2014**, *6*, 10593 – 10601.

[80] a) V. C. Tung, L.-M. Chen, M. J. Allen, J. K. Wassei, K. Nelson, R. B. Kaner, Y. Yang, *Nano Lett.* **2009**, *9*, 1949 – 1955; b) S. Watcharotone, D. A. Dikin, S. Stankovich, R. Piner, I. Jung, G. H. B. Dommett, G. Evmenenko, S.-E. Wu, S.-F. Chen, C.-P. Liu, S. T. Nguyen, R. S. Ruoff, *Nano Lett.* **2007**, *7*, 1888 – 1892; c) J. S. Woo, J. T. Han, S. Jung, J. I. Jang, H. Y. Kim, H. J. Jeong, S. Y. Jeong, K.-J. Baeg, G.-W. Lee, *Sci. Rep.* **2014**, *4*, 4804; d) S. Tuukkanen, M. Hoikkanen, M. Poikelispaa, M. Honkanen, T. Vuorinen, M. Kakkonen, J. Vuorinen, D. Lupo, *Synth. Met.* **2014**, *191*, 28 – 35; e) H. Chang, G. Wang, A. Yang, X. Tao, X. Liu, Y. Shen, Z. Zheng, *Adv. Funct. Mater.* **2010**, *20*, 2893 – 2902; f) D. Y. Choi, H. W. Kang, H. J. Sung, S. S. Kim, *Nanoscale* **2013**, *5*, 977 – 983.

[81] P. Lee, J. Ham, J. Lee, S. Hong, S. Han, Y. D. Suh, S. E. Lee, J. Yeo, S. S. Lee, D. Lee, S. H. Ko, *Adv. Funct. Mater.* **2014**, *24*, 5671 – 5678.

[82] R. Chen, S. R. Das, C. Jeong, M. R. Khan, D. B. Janes, M. A. Alam, *Adv. Funct. Mater.* **2013**, *23*, 5150 – 5158.

[83] M.-S. Lee, K. Lee, S.-Y. Kim, H. Lee, J. Park, K.-H. Choi, H.-K. Kim, D.-G. Kim, D.-Y. Lee, S. Nam, J.-U. Park, *Nano Lett.* **2013**, *13*, 2814 – 2821.

[84] I. K. Moon, J. I. Kim, H. Lee, K. Hur, W. C. Kim, H. Lee, *Sci. Rep.* **2013**, *3*, 1112.

[85] H. J. Lee, J. H. Hwang, K. B. Choi, S.-G. Jung, K. N. Kim, Y. S. Shim, C. H. Park, Y. W. Park, B.-K. Ju, *ACS Appl. Mater. Interfaces* **2013**, *5*, 10397 – 10403.

[86] C. H. Chung, T. B. Song, B. Bob, R. Zhu, Y. Yang, *Nano Res.* **2012**, *5*, 805 – 814.

[87] J. Liang, L. Li, K. Tong, Z. Ren, W. Hu, X. Niu, Y. Chen, Q. Pei, *ACS Nano* **2014**, *8*, 1590 – 1600.

[88] Z. Liu, K. Parvez, R. Li, R. Dong, X. Feng, K. Müllen, *Adv. Mater.* **2015**, *27*, 669 – 675.

Received: February 9, 2015
Published online: July 16, 2015

  